FEBS Letters 580 (2006) 982–987

Binding of different monosaccharides by lectin PA-IIL from *Pseudomonas aeruginosa*: Thermodynamics data correlated with X-ray structures

Charles Sabin[a,b], Edward P. Mitchell[b], Martina Pokorná[c], Catherine Gautier[a], Jean-Pierre Utille[a], Michaela Wimmerová[c], Anne Imberty[a,*]

[a] *CERMAV-CNRS (affiliated with Université Joseph Fourier), 601 rue de la Chimie, Grenoble BP53, F-38041 Grenoble cedex 09, France*
[b] *E.S.R.F. Experiments Division, BP-220, F-38043 Grenoble cedex 09, France*
[c] *National Centre for Biomolecular Research and Department of Biochemistry, Masaryk University, Kotlarska 2, 611 37 Brno, Czech Republic*

Received 9 December 2005; revised 10 January 2006; accepted 12 January 2006

Available online 19 January 2006

Edited by Irmgard Sinning

Abstract The lectin from *Pseudomonas aeruginosa* (PA-IIL) is involved in host recognition and biofilm formation. Lectin not only displays an unusually high affinity for fucose but also binds to L-fucose, L-galactose and D-arabinose that differ only by the group at position 5 of the sugar ring. Isothermal calorimetry experiments provided precise determination of affinity for the three methyl-glycosides and revealed a large enthalpy contribution. The crystal structures of the complexes of PA-IIL with L-galactose and Met-β-D-arabinoside have been determined and compared with the PA-IIL/fucose complex described previously. A combination of the structures and thermodynamics provided clues for the role of the hydrophobic group in affinity.

Keywords: Lectin; Cystic fibrosis; Crystal structure; Thermodynamics; Galactose; Arabinose; *Pseudomonas aeruginosa*

1. Introduction

Pseudomonas aeruginosa is a gram negative bacterium and an opportunistic pathogen that infects immunocompromised patients and which is often involved in nosocomial infections. The bacterium is also responsible for chronic respiratory tract infections of individuals under mechanical ventilation and patients suffering from cystic fibrosis (CF). Carbohydrates play an important role in infections, since they are a target for bacterial binding through virulence factors such as adhesions, present on pili or flagella, and soluble lectins [1]. In the particular case of CF lungs, an increase of fucosylation is observed, both at the levels of epithelia glycoconjugates [2] and altered mucins [3], and a fucose binding lectin from *P. aeruginosa* (PA-IIL) has been demonstrated to bind specifically to CF airline culture cells [4]. The tetrameric lectin that was first identified and characterised from *P. aeruginosa* cytoplasm [5] has been shown to be present in large quantities on the outer membrane of the bacteria and to also be involved in biofilm formation [6].

Through protein crystallography at high resolution, a precise three-dimensional knowledge of lectin has allowed the structural basis of the interaction between PA-IIL and fucose and fucose-containing oligosaccharides to be understood [7,8]. An unusual binding mode, mediated by two calcium ions, is responsible for the micromolar affinity for fucose which is much higher than that classically observed in protein/carbohydrate interactions [9]. Previous inhibition tests have demonstrated that other monosaccharides are also recognised by PA-IIL with affinity (strongest first) L-fucose (Fuc) > L-galactose (L-Gal) > D-arabinose (Ara) > D-fructose (Fru) > D-mannose (Man) [10]. Indeed, these monosaccharides all have either an L-*galacto* or a D-*manno* configuration that contains two equatorial and one axial hydroxyl groups when in the $^{1}C_{4}$ and $^{4}C_{1}$ pyranose conformation, respectively. This set of groups are needed for the coordination of the two calcium ions (Fig. 1) as was observed in the X-ray crystal structures of the PA-IIL complexes with mannose and fructose [11].

In the present work, we focus on comparing the binding modes of the three monosaccharides with highest affinity for PA-IIL, i.e. Fuc, L-Gal and Ara, that differ only by the nature of the group at C5 (Fig. 1). Precise equilibrium association constants, together with their enthalpic and entropic contributions, were evaluated for PA-IIL interacting with these monosaccharides and two additional crystal structures have been determined at very high resolution for the complexes involving L-Gal and Ara. Such studies can provide the basis for designing higher affinity ligands that could be of therapeutic interest as antibacterial compounds.

2. Materials and methods

Recombinant PA-IIL was purified from *Escherichia coli* BL21(DE3) containing the plasmid pET25pa2l as described previously [9]. Fuc, Man, β-methyl-D-arabinopyranoside (Me-β-Ara) and α-methyl-D-mannopyranoside (Me-α-Man) were purchased from Sigma. α-Methyl-L-fucopyranoside (Me-α-Fuc) was purchased from Interchim. L-Gal was either purchased from Sigma or Institute of Chemistry (Bratislava) or prepared from L-galactono-1,4-lactone (Fluka) by preparing 1,2,3,4,6-penta-*O*-acetyl-L-galactose according to Thiem et al. [12] followed by deacetylation using the conventional

*Corresponding author. Fax : +33 476 54 72 03.
E-mail address: imberty@cermav.cnrs.fr (A. Imberty).

Abbreviations: PA-IIL, lectin II from *Pseudomonas aeruginosa*; CF, cystic fibrosis; L-Gal, L-galactose; Fuc, L-fucose; Man, D-mannose; Ara, D-arabinose; Me-α-L-Gal, α-methyl-L-galactopyranoside; Me-α-Fuc, α-methyl-L-fucopyranoside; Me-α-Man, α-methyl-D-mannopyranoside; Me-β-Ara, β-methyl-D-arabinopyranoside

0014-5793/$32.00
doi:10.1016/j.febslet.2006.01.030

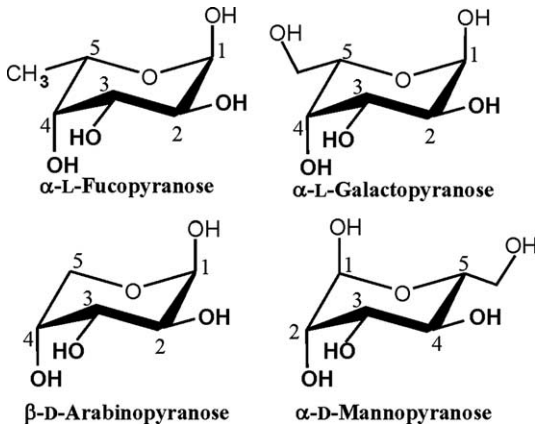

Fig. 1. Schematic representation of the monosaccharides of interest together with numbering of ring carbons. The three hydroxyl groups involved in the coordination of calcium when complexed with PA-IIL are indicated in bold.

Zemplèn reaction (MeO^-Na^+ 1 M in MeOH). α-Methyl-L-galactopyranoside (Me-α-L-Gal) was synthesised from L-Gal with the following procedure: Me-L-galactoside isomers were prepared by refluxing L-Gal in dry MeOH in the presence of BF3 etherate for 15 h. Silica gel chromatography led to the separation of pure Me-α-L-Gal; ^{1}H NMR of the acetylated derivative showed a coupling constant $J_{1,2}$ = 3.66 Hz in agreement with an α-L-configuration [12]. ^{13}C NMR (D_2O, 75 MHz): 100.41 (C1), 71.74, 70.47, 70.26, 69.19 (C2,C3,C4,C5), 62.25 (C6), 56.06 (OCH_3).

Isothermal calorimetry (ITC) experiments were carried out at 25 °C with a VP-ITC calorimeter from Microcal (Northampton, MA). Proteins and sugars were dissolved in the same buffer (0.1 M Tris–HCl with 0.03 mM $CaCl_2$ at pH 7.5, filtered through 0.22 μm ∅). The protein concentration in the microcalorimeter cell (1.4 ml) varied from 0.05 to 0.3 mM in order to keep the C value between 5 and 100 (where $C = K_a M$, where M is the initial concentration of the macromolecule). A total of 30 injections of 10 μl of sugar solution at concentrations varying from 0.4 to 3 mM were added at intervals of 5 min whilst stirring at 310 rpm. Control experiments yielded insignificant heats of dilution. The thermodynamic parameters n, K_a and ΔH were obtained by fitting the classical titration curve [13] to experimental data using Origin7.0 software (Microcal).

The crystals were grown using the hanging drop vapour diffusion method and Hampton Screens I and II (Hampton Research) at 20 °C. The best results were obtained using 2.5 μl of lyophilised purified PA-IIL dissolved in water (10 mg ml^{-1}) in the presence of Me-β-Ara or L-Gal (250 μg ml^{-1}) and $CaCl_2$ salt (2 mM) mixed with 2.5 μl of the reservoir solution consisting of 1.75 M ammonium sulfate in 0.1 M Tris–HCl, pH 8.5. Crystals of both complexes were cryo-cooled to 100 K, after soaking them for as short a time as possible in 25% glycerol v/v in the precipitant solution. All data images were recorded on an ADSC Q4R CCD detector (Quantum corp.) using X-rays of 0.93 Å wavelength on beamline ID14-1 or ID14-4 at the ESRF (Grenoble, France). The data were processed with MOSFLM [14] and scaled and converted to structure factors using the CCP4 programme suite [15] (Table 1).

The phases were first determined by the molecular replacement technique with the MOLREP program of CCP4 using the monomeric PA-IIL/Fuc structure (PDB code 1UZV) [9] stripped of water molecules, calcium ions and sugar ligands as the search probe. Four clear solutions were found for both complexes, resulting in tetramers in the asymmetric units. Initial structures were entirely rebuilt automatically using ARP/warp [16] and clear electron density could be observed for the monosaccharides (Fig. 2). Refinement was performed with REFMAC [17]. Alternating cycles of refinement with manual construction using O [18] of missing residues, alternative conformations, water molecules, calcium ions and sugar ligands resulted in the final structures. Coordinates and structure factors of the PA-IIL complexes with L-Gal and Me-β-Ara have been deposited in the Protein Data Bank under codes 2BP6 and 2BOJ, respectively.

Table 1
Data collection and refinement statistics

	PA-IIL/Me-β-Ara	PA-IIL/Me-α-L-Gal
Data collection		
Beamline (ESRF)	ID14-2	ID14-4
Wavelength (Å)	0.933	0.932
Resolution range (Å)	1.8–30.0	1.5–19.4
Highest resolution shell (Å)	1.80–1.90	1.50–1.55
Space group	$P2_1$	$P2_1$
Cell dimensions		
a (Å)	50.64	52.63
b (Å)	80.17	54.53
c (Å)	52.52	94.38
β (°)	109.92	94.38
Matthews coef (Å^3/DA)	1.74	1.90
Solvent content (%)	29	35
Measured reflections	133 138	213 637
Unique reflections	35 769	63 528
Average multiplicity[a]	3.73 (3.45)	3.82 (3.80)
Completeness[a] (%)	97.9 (89.0)	96.8 (95.1)
Average[a] $I/\sigma I$	7.50 (3.64)	10.35 (3.08)
R merge[a,b] (%)	7.4 (19.0)	5.0 (23.0)
Wilson B-factor (Å^2)	11.4	10.3
Refinement		
R_{crys}[c] (no. of observations)	0.137 (34 653)	0.143 (61 594)
R_{free}[d] (no. of observations)	0.172 (1116)	0.166 (1934)
RMS deviation from ideality		
Bonds (Å)	0.011	0.012
Angles (°)	1.320	1.398
Total number of atoms:		
Protein	3308	3308
Ligand	44	66
Calcium	8	8
Water	612	430
Average refined B-factors per chains (A/B/C/D)		
Protein	8.6/9.5/9.7/8.3	8.4/10.1/10.0/8.9
Ligand	7.7/10.8/10.6/7.9	6.5/8.8/8.3/8.3
Calcium	6.4/8.5/6.7/8.7	5.9/6.9/6.0/6.0
Water	25.3/26.2/25.1/26.2	22.4/ 22.9/23.5/21.9
Number of side chains modelled with alternative conformations	17 Chain A: S23, K62, V81 Chain B: V54, V77, V81 Chain C: S23, T39, Q53, V81, E86 Chain D: S23, T39, N70, V77, V81, E86	16 Chain A: S23, L31, N46, S68, V77, V81 Chain B: S59, V77, V81, I82 Chain C: N29 , S41, S77 Chain D: N46, V77, V81
PDB deposition code	2BOJ	2BP6

[a]Numbers in parentheses refer to the highest resolution shell.
[b]$R_{merge} = \sum|I - \langle I\rangle|/\sum\langle I\rangle$, where I = observed intensity.
[c]$R_{cryst} = \sum||F_o| - |F_c||/\sum|F_o|$, where $|F_o|$ = observed structure factor amplitude and $|F_c|$ = calculated structure factor amplitude.
[d]R_{free} is R_{cryst} for 3% of reflections excluded from the refinement.

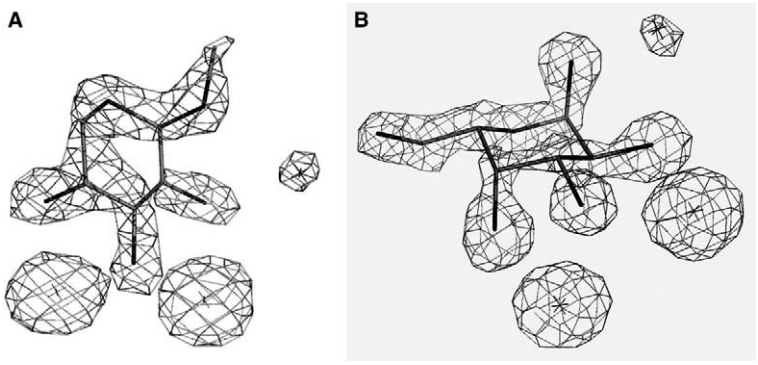

Fig. 2. Initial sigma-weighted F_o–F_c electron density map. (A) The map has been contoured at 3σ around the Met-β-D-arabinopyranoside in the PA-IIL–Me-β-D-Ara complex calculated after molecular replacement and after the first cycle of refinement without ligand and water molecules. (B) Same representation for the L-Gal in the PA-IIL–L-Gal complex. The final positions of the monosaccharides, calcium and water in the model have been superimposed as stick representation for comparison. Molecular drawings were prepared with Pymol (DeLano Scientific LLC).

3. Results

3.1. Thermodynamics of PA-IIL binding to monosaccharides

Thermodynamic data were recorded for the interaction of PA-IIL with methyl-glycosides of the monosaccharides of interest, i.e. Me-α-L-Gal, Me-β-Ara and also Me-α-Fuc and Me-α-Man for comparison. The use of methyl derivatives avoids the problems related to anomeric disorder in solution and also gives a better mimic of real biological interactions where the monosaccharides are not free but linked to glycoconjugates.

A typical titration curve of PA-IIL interacting with Me-α-Fuc is shown in Fig. 3. The thermodynamic parameters are reported in Table 2. The stoichiometry of binding is usually close to 1, whilst some protein batches occasionally display lower values (minimum 0.75). Nevertheless, the other binding constants are not affected by the variation in stoichiometry. The affinity is maximal for binding to Me-α-Fuc with a dissociation constant of 430 nM. The affinity for the methyl-fucoside is 10-fold higher than for the unmodified sugar, an effect that is usually observed in protein–carbohydrate interactions. The qualitative order of preference that was observed by inhibition of haemagglutination experiments [10] is confirmed by the present data. Quantitatively, PA-IIL affinity for Me-α-Fuc is threefold stronger than for Me-α-L-Gal and Me-β-Ara and 140-fold better than for Me-α-Man.

All complexes formed here are driven by enthalpy. The interaction of the lectin with monosaccharides of the L-*galacto* configuration gives a higher enthalpy of binding ($\Delta H < -30$ kJ/mol) than for mannose ($\Delta H = -20$ kJ/mol). The PA-IIL/Me-α-Fuc complex has the highest enthalpy of binding with $\Delta H = -40$ kJ/mol. The entropy contribution $-T\Delta S$ can be slightly unfavourable, as in the case of Me-α-Fuc and Me-β-Ara, or slightly favourable, as in the case of Me-α-L-Gal and Me-α -Man, but it is always a low contribution with a maximum of 17% of the free energy of binding.

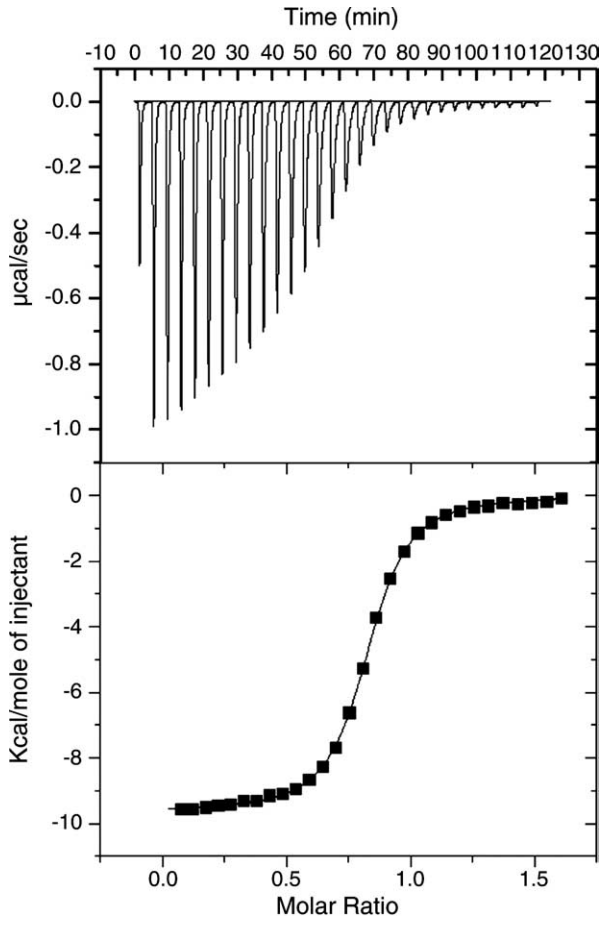

Fig. 3. Titration microcalorimetry results of Me-α-Fuc (0.44 mM) binding to PA-IIL (55.8 μM) in 100 mM Tris buffer, pH 7.5, with 0.03 mM $CaCl_2$. Top: data obtained from 30 automatic injections (10 μl) of Me-α-Fuc each into the cell containing PA-IIL. Lower: plot of the total heat released as a function of total ligand concentration for the titration shown in the upper panel. The solid line represents the best least-squares fit for the obtained data.

3.2. Crystal structure of PA-IIL/L-Gal complex

The overall structure of the PA-IIL complex with L-Gal to 1.4 Å resolution is similar to the PA-IIL/Fuc complex determined previously [7,9]. All 114 amino acids can be observed together with the two calcium ions and the monosaccharide of each subunit of the tetramer (Fig. 4). Two sulfate ions and 430 water molecules were incorporated in the model. The monomer is a β-sandwich composed of 8 antiparallel strands of which the first five are arranged in Greek key and which form an acidic pocket allowing the binding of two intimate Ca^{2+} ions (3.75 Å separation). The amino acids

Table 2
Thermodynamics–ITC data for different monosaccharides interacting with PA-IIL[a]

	Ka 10^4 M^{-1}	Kd 10^{-6} M	*n*	$-\Delta G$ (kJ/mol)	$-\Delta H$ (kJ/mol)	$-T\Delta S$ (kJ/mol)
L-Fuc[b]	34 (±3)	2.9 (±0.03)	0.96 (±0.04)	31.5 (±0.2)	31.2 (±0.1)	−0.3 (±0.1)
Me-α-Fuc	235 (±8)	0.43 (±0.01)	0.77 (±0.03)	36.4 (±0.1)	41.3 (±1)	4.9 (±1)
Me-α-L-Gal	85 (±5)	1.17 (±0.07)	0.90 (±0.04)	33.8 (±0.1)	31.5 (±0.6)	−2.3 (±0.7)
Me-β-Ara	60 (±5)	1.7 (±0.1)	1.10 (±0.03)	33.0 (±0.2)	37.9 (±0.8)	5.4 (±1.0)
Me-α-Man	1.42 (±0.05)	71 (±3)	0.94 (±0.01)	23.7 (±0.1)	17.8 (±0.4)	−5.9 (±0.3)

[a]Values in parentheses are standard deviations from three separate isothermal titrations.
[b]Taken from Perret et al. [8].

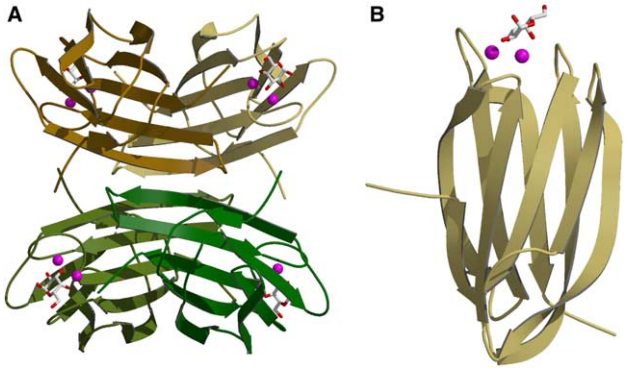

Fig. 4. Ribbon representation of the PA-II lectin/L-Gal complex. (A) Tetramer consisting of the asymmetric unit with stick representation of L-Gal ligand and cpk representation of the calcium ions. (B) Same representation for the monomer. Molecular drawings were prepared with MOLSCRIPT [23] and RASTER-3D [24].

of the pocket, Asn21, Glu95, Asp99, Asp101, Asn103, Asp104, as well as the Gly114* terminus of the adjacent monomer, complete a large part of the coordination sphere of the two calcium ions (Fig. 5). One calcium ion is coordinated by five oxygen atoms from carboxylate groups and two from the sugar ligand, whereas the other calcium receives three oxygen atoms from carboxylate groups, two from carbonyl groups and two from the sugar ligand. The sugar ring oxygen O5 forms a hydrogen bond with the NH backbone group of Ser23. One water molecule plays a special role by bridging between the L-Gal oxygen atoms O1 and O2 and the main chain NH groups of residues Thr98 and Asp99. Details of distances are listed in Table 3.

The hydroxymethyl group of L-Gal is tucked into a shallow cavity with amphiphilic character between Thr45 and Ser23. The CH2 group at C6 makes hydrophobic contacts with the methyl group of Thr45. Some conformational disorder is observed for the O6 atom of the hydroxymethyl group. In three of the four binding sites, the O6 atom is in the *gauche-trans* (*gt*) conformation (relative to O5 and C4 [19]) and makes a hydrogen bond to a water molecule. This water molecule does not bridge directly to the protein but is part of a complex network with variations between the binding sites. In the fourth binding site (chain A), the hydroxymethyl group adopts another conformation, referred to as *trans-gauche* (*tg*), and makes contact to another water molecule. These two rotamers of the hydroxymethyl group of galactose have been reported to be the two most populated ones, both in the crystalline state [19] and in water solution [20]. Interestingly, this alternative conformation makes some free space for the hydroxyl group of Ser23 that becomes flexible and adopts two alternative conformations.

3.3. Crystal structure of PA-IIL /Me-β-Ara complex

The crystal structure of the PA-IIL complex with Me-β-Ara is isomorphous to those of PA-IIL/Fuc and PA-IIL/L-Gal and the overall tetrameric structures are similar. In addition to eight calcium ions and four Me-β-Ara ligands, one sulfate and 612 water molecules could be located in the electron density map. The orientation of the Me-β-Ara ring in the binding site is similar to that of L-Gal described above (Fig. 5 and Table 3). The ring carbon atom C-5 does not carry any substituent and therefore leaves an empty space between Thr45 and Ser23 side chains. As a result, the hydroxyl group of Ser23 adopts two alternative conformations in all binding sites except in chain B.

4. Discussion

A comparison of the two crystal structures described here to that reported previously for the PA-IIL/Fuc complex [9] allows the particular role of the moiety at position 5 of the ring to be explored. Indeed, all other contacts between the protein and the monosaccharides are identical in the different complexes and the differences in binding affinity must therefore be correlated with this particular group.

In terms of affinity, the present study highlights the important contribution of hydrophobic contacts. In general, interactions between proteins and carbohydrates present a balance of hydrogen bonds and hydrophobic contacts. PA-IIL is a rather unique case since its interaction with fucose is established mainly through coordination by calcium ions and hydrogen bonds. The only hydrophobic interaction is established between the methyl group at C5 of fucose and the side chain of Thr45. When this interaction is weakened, as in the complex with L-Gal, or absent, as with Me-β-Ara, the affinity is decreased by 3-fold.

The relative contributions of the different thermodynamic parameters are more difficult to rationalise. The entropic term is the sum of multiple effects. A favourable entropic contribution is obtained when the increase of solvent entropy coming from water driven out of the site is correlated with minimal loss of conformational degrees of freedom in either ligand or protein chains during binding. This is not usually the case in protein-carbohydrate interactions where a strong entropy barrier is usually observed [21,22].

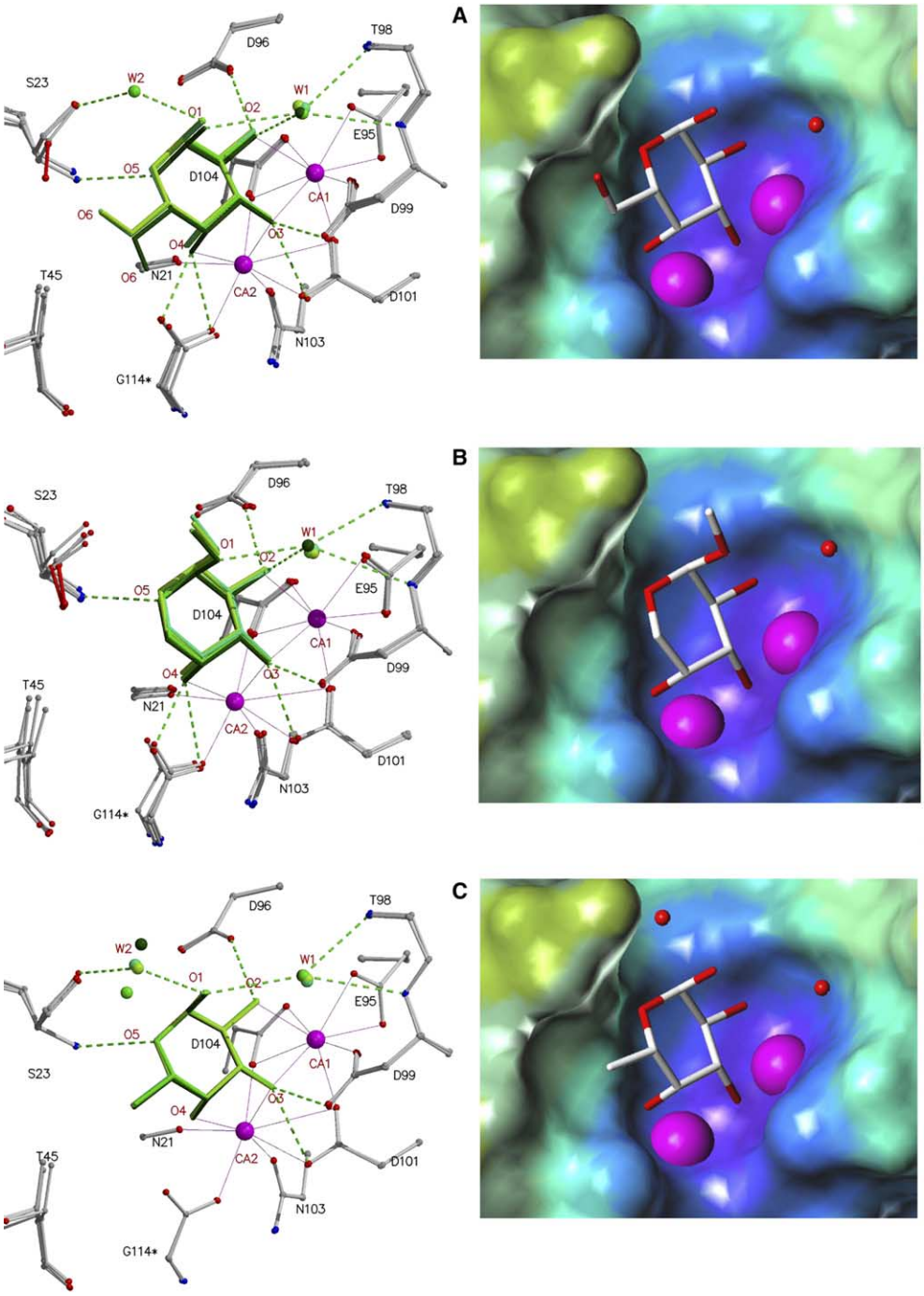

Fig. 5. Binding sites of PA-IIL complexed with monosaccharides. *Left panel*: superposition of the four binding sites of the asymmetric unit. Sugar and water molecules belonging to the same monomer are drawn with the same shade of green. Coordination contacts are indicated by blue solid lines and hydrogen bonds by green dashed lines. The * symbol indicates the terminal glycine from the second monomer. *Right panel*: Accessible surface of the protein calculated with the MOLCAD program [25] for one binding site. (A) PA-IIL/L-Gal complex, (B) PA-IIL/Me-β-Ara complex, (C) PA-IIL/Fuc complex from PDB code 1UZV [9].

However, in the sugar free structure of PA-IIL [11] three water molecules strongly coordinated to the calcium ions replace the three hydroxyl groups O2, O3 and O4 of the fucose complex. The release of these water molecules that are more strongly bound than in a classical carbohydrate binding site can explain the absence of a strong entropy barrier for the PA-IIL/monosaccharide interaction. In our study, galactoside and mannoside are the two glycosides with favourable entropy of binding and this observation may be correlated to the conformational flexibility of the O6 hydroxyl group, as observed in the X-ray structures of both complexes.

Table 3
Comparison of contact distances in Å the PA-IIL binding site[a]

		PA-IIL/ Fuc[b]	PA-IIL/ Me-β-Ara	PA-IIL/ L-Gal
Calcium coordination				
Ca-1	O2	2.50	2.53	2.51
Ca-1	O3	2.48	2.50	2.49
Ca-2	O3	2.48	2.46	2.46
Ca-2	O4	2.49	2.52	2.50
Hydrogen bonds				
Asp96.OD1	O2	2.65	2.63	2.62
Asp 99.OD1	O3	2.98	2.99	3.00
Asp 99.OD2	O3	2.56	2.54	2.57
Asp 101.OD1	O3	2.95	2.97	2.94
Asp 101.OD2	O3	2.93	2.92	2.92
Asp 104.OD2	O3	3.00	3.03	3.05
Asn 21.O	O4	3.07	3.01	3.02
Gly 114*.OXT[c]	O4	2.56	2.47	2.51
Ser23. N	O5	2.95	2.93	2.95
Wat_1[d]	O1	3.2	3.03	3.17
Wat_1	O2	3.05	3.02	3.05
Wat_2[e]	O1	3.05	–	2.84
Hydrophobic contacts				
Thr45.CG2	$C6_{Me}$	4.12	–	4.08

[a]Distances given are a mean from the distances observed in the four independent molecules in the asymmetric unit.
[b]Values taken from PDB structure 1UZV [9].
[c]C-terminal residue from neighbouring monomer.
[d]Water bridging to Thr98.NH and Asp99.NH.
[e]Water bridging to Ser23.OH.

Acknowledgements: The help of Jan Adam is acknowledged for microcalorimetry experiments. We thank the ESRF, Grenoble, for access to synchrotron data collection facilities. The work was supported by Ministry of Education of The Czech Republic (Contract MSM0021622413), by CNRS, by French Ministry of Research ACI Microbiologie program, by the Mizutani Foundation for Glycosciences and by French Association Vaincre la Mucoviscidose.

References

[1] Imberty, A., Mitchell, E.P. and Wimmerová, M. (2005) Structural basis for high affinity glycan recognition by bacterial and fungal lectins. Curr. Opin. Struct. Biol. 15, 525–534.
[2] Rhim, A.D., Stoykova, L.I., Trindade, A.J., Glick, M.C. and Scanlin, T.F. (2004) Altered terminal glycosylation and the pathophysiology of CF lung disease. J. Cyst. Fibros. 3, 95–96.
[3] Roussel, P. and Lamblin, G. (2003) The glycosylation of airway mucins in cystic fibrosis and its relationship with lung infection by *Pseudomonas aeruginosa*. Adv. Exp. Med. Biol. 535, 17–32.
[4] Stoykova, L.I., Ellway, J., Rhim, A.D., Kim, D.J., Hlick, M.C. and Scanlin, T.F. (2005) Binding of *Pseudomonas aeruginosa* lectin LecB to cystic fibrosis airwat cells is inhibited by fucosylated compounds: implication for therapy, in: Proceedings of the 2005 Annual Conference of the Society for Glycobiology, no. 169. Glycobiology 15, 1228.
[5] Gilboa-Garber, N. (1982) *Pseudomonas aeruginosa* lectins. Method. Enzymol. 83, 378–385.
[6] Tielker, D., Hacker, S., Loris, R., Strathmann, M., Wingender, J., Wilhelm, S., Rosenau, F. and Jaeger, K.-E. (2005) *Pseudomonas aeruginosa* lectin LecB is located in the outer membrane and is involved in biofilm formation. Microbiology 151, 1313–1323.
[7] Mitchell, E. et al. (2002) Structural basis for oligosaccharide-mediated adhesion of *Pseudomonas aeruginosa* in the lungs of cystic fibrosis patients. Nat. Struct. Biol. 9, 918–921.
[8] Perret, S. et al. (2005) Structural basis for the interaction between human milk oligosaccharides and the bacterial lectin PA-IIL of *Pseudomonas aeruginosa*. Biochem. J. 389, 325–332.
[9] Mitchell, E.P. et al. (2005) High affinity fucose binding of *Pseudomonas aeruginosa* lectin PA-IIL: 1.0 Å resolution crystal structure of the complex combined with thermodynamics and computational chemistry approaches. Proteins: Struct. Funct. Bioinfo. 58, 735–748.
[10] Garber, N., Guempel, U., Gilboa-Garber, N. and Doyle, R.J. (1987) Specificity of the fucose-binding lectin of *Pseudomonas aeruginosa*. FEMS Microbiol. Lett. 48, 331–334.
[11] Loris, R., Tielker, D., Jaeger, K.-E. and Wyns, L. (2003) Structural basis of carbohydrate recognition by the lectin LecB from *Pseudomonas aeruginosa*. J. Mol. Biol. 331, 861–870.
[12] Binch, H., Stangier, K. and Thiem, J. (1998) Chemical synthesis of GDP-L-galactose and analogues. Carbohydr. Res. 306, 409–419.
[13] Wiseman, T., Williston, S., Brandts, J.F. and Lin, L.N. (1989) Rapid measurement of binding constants and heats of binding using a new titration calorimeter. Anal. Biochem. 179, 131–137.
[14] Leslie, A.G.W. (1992) Recent changes to the MOSFLM package for processing film and image plate data. Joint CCP4 + ESF-EAMCB Newsletter on Protein Crystallography 26.
[15] Collaborative Computational Project Number 4 (1994) The CCP4 suite: programs for protein crystallography. Acta Crystallogr. D 50, 760–763.
[16] Perrakis, A., Morris, R. and Lamzin, V.S. (1999) Automated protein model building combined with iterative structure refinement. Nat. Struct. Biol. 6, 458–463.
[17] Murshudov, G.N., Vagin, A.A. and Dodson, E.J. (1997) Refinement of macromolecular structures by the maximum-likelihood method. Acta Crystallogr. D 53, 240–255.
[18] Jones, T.A., Zou, J.Y., Cowan, S.W. and Kjeldgaard, M. (1991) Improved methods for the building of protein models in electron density maps and the location of errors in these models. Acta Crystallogr. A 47, 110–119.
[19] Marchessault, R.H. and Pérez, S. (1979) Conformations of the hydroxymethyl group in crystalline aldohexopyranoses. Biopolymers 18, 2369–2374.
[20] Nishida, Y., Ohrui, H. and Meguro, H. (1984) Proton NMR studies of (6R)- and (6S)-deuterated D-hexoses: assignment of the preferred rotamers about C5–C6 bond of D-glucose and D-galactose derivatives in solutions. Tetrahedron Lett. 25, 1575–1578.
[21] Carver, J.P. (1993) Oligosaccharides: how flexible molecules can act as signals. Pure Appl. Chem. 65, 763–770.
[22] Dam, T.K. and Brewer, C.F. (2002) Thermodynamic studies of lectin-carbohydrate interactions by isothermal titration calorimetry. Chem. Rev. 102, 387–429.
[23] Kraulis, P. (1991) Molscript: a program to produce both detailed and schematic plots of protein structures. J. Appl. Crystallogr. 24, 946–950.
[24] Merrit, E.A. and Murphy, M.E. (1994) Raster3D version 2.0. A program for photorealistic molecular graphics. Acta Crystallogr. D 50, 869–873.
[25] Waldherr-Teschner, M., Goetze, T., Heiden, W., Knoblauch, M., Vollhardt, H. and Brickmann, J. (1992) MOLCAD – computer aided visualization and manipulation of models in molecular science in: Advances in Scientific Visualization (Post, F.H. and Hin, A.J.S., Eds.), pp. 58–67, Springer, Heidelberg.